

# Chromium tricarbonyl complexes of 1,2- and 1,4-dihydronaphthalene. Synthesis and metal-induced thermal isomerizations involving *endo*-hydrogen atoms

Yu. F. Oprunenko,\* I. P. Gloriozov, and D. A. Lemenovskii

Department of Chemistry, M. V. Lomonosov Moscow State University,  
1 Leninskie Gory, 119992 Moscow, Russian Federation.

Fax: +7 (495) 932 8846. E-mail: oprunenko@nmr.chem.msu.su

Reactions of 1,4-dihydronaphthalene with  $(\text{NH}_3)_3\text{Cr}(\text{CO})_3$  or  $\text{Py}_3\text{Cr}(\text{CO})_3$  in the presence of  $\text{BF}_3 \cdot \text{Et}_2\text{O}$  afford a mixture of isomeric  $\eta^6$ -chromium tricarbonyl complexes of 1,4- and 1,2-dihydronaphthalene in the ratio 63 : 37 and 55 : 45, respectively. The complexes were separated by chromatography. At 130 °C in different solvents these complexes undergo thermally induced reversible rearrangement studied by the  $^2\text{H}$  NMR method for the deuterated derivatives. Analysis of the  $^2\text{H}$  NMR spectra showed that the isomerization occurs due to metal-induced 1,5-shifts of the *endo*-hydrogen atoms. The isomerization mechanism was studied by quantum chemical DFT calculations. The calculations showed that the process occurs with the maximum activation barrier (33.2 kcal mol $^{-1}$ ) through a series of agostic and hydride intermediates and transition states in which the chromium atom stereospecifically activates the *endo*-hydrogen atoms only.

**Key words:** chromium tricarbonyl complexes, dihydronaphthalenes, lithiation, 1,5-hydride shift, haptotropic rearrangements, quantum chemical calculations, density functional theory.

Reactions of isomeric 1,4- and 1,2-dihydronaphthalenes containing both aromatic and cyclohexadiene rings with complex chromium carbonyls  $\text{L}_3\text{Cr}(\text{CO})_3$  should afford the corresponding chromium tricarbonyl  $\eta^6$ -complexes **1** and **2** to the benzene ring.<sup>1</sup> However, coordination of the  $\text{Cr}(\text{CO})_3$  group (in the general case,  $\text{CrL}_3$ ) is also possible to the second, formally cyclohexadiene ring containing two  $\text{sp}^3$ -hybridized carbon atoms and two double bonds. This coordination can provide agostic and/or hydride complexes. Rather stable monocyclic cyclohexadiene complexes of this type are known.<sup>2–5</sup>

It can be assumed that the tricarbonylchromium group in polycyclic complexes **1** and **2** can migrate from the arene to cyclohexadiene ring due to thermally induced inter-ring haptotropic rearrangements (IRHR).<sup>1</sup> The driving force of this process could be the formation of coordinately saturated hydride and agostic complexes. This rearrangement can be accompanied by shifts of hydrogen atoms involving no transition metal<sup>3</sup> or induced by the metal through the formation of hydride<sup>4</sup> and agostic<sup>5</sup> intermediates, which finally results in the isomerization of an organic ligand in the coordination sphere of the transition metal. In the complexes with monocyclic ligands, for instance, cyclohexadiene or cycloheptatriene, participa-

tion of the transition metal in hydride shifts of hydrogen atoms resulting in ligand isomerization due to migration of the *endo*-H atoms only has been proved rather strictly.<sup>3–6</sup>

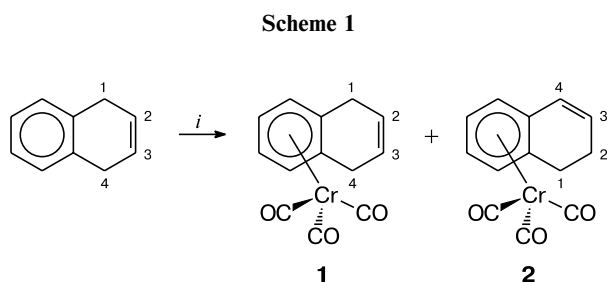
We have earlier<sup>6</sup> proposed IRHR of this type with presumable participation of hydride and agostic intermediates to explain the *endo*-hydride shifts in the chromium tricarbonyl complexes of 1,6-methano[10]annulene derivatives. We also found another mechanism of hydride shifts in the complexes of polycyclic aromatic compounds and showed that in the chromium tricarbonyl complexes of phenalene, which is formally a vinyl-substituted arene, hydride shifts are observed for both *endo*- and *exo*-hydrogen atoms, *i.e.*, occur, probably, involving no chromium atom.<sup>2</sup> Reasons for so different behavior of structurally related complexes remain unclear.

Thus, the chromium tricarbonyl complexes of dihydronaphthalenes and other polycyclic arylalkenes are promising models for revealing new types of the dynamic behavior of organometallic compounds.

## Results and Discussion

The reaction of 1,4-dihydronaphthalene with the triammonia complex  $(\text{NH}_3)_3\text{Cr}(\text{CO})_3$  for 2 h at 100 °C in

dioxane or with the tris-pyridine complex  $\text{Py}_3\text{Cr(CO)}_3$  for 1 h at  $-30^\circ\text{C}$  in ether in the presence of boron trifluoride etherate affords a mixture of ( $\eta^6$ -dihydronaphthalene)chromium tricarbonyl complexes **1** and **2** in 45 and 50% yield and the ratio **1** : **2** = 63 : 37 and 55 : 45, respectively (Scheme 1).



*i.*  $(\text{NH}_3)_3\text{Cr(CO)}_3$  or  $\text{Py}_3\text{Cr(CO)}_3$ .

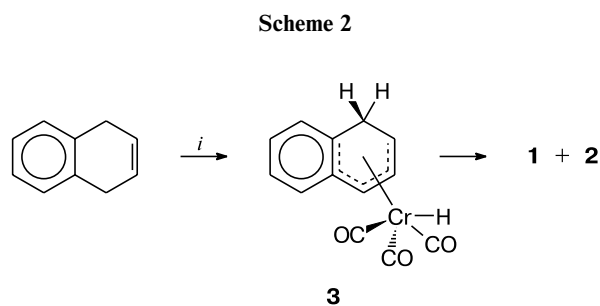
Complexes **1** and **2** were separated by TLC. According to published data,<sup>7</sup> the reaction of isomeric 1,2-dihydronaphthalene with  $(\text{NH}_3)_3\text{Cr(CO)}_3$  affords only complex **2**.

Thus, under rather mild conditions, the complex formation of 1,4-dihydronaphthalene is accompanied by isomerization to 1,2-dihydronaphthalene, which is an important initial compound in synthesis of anthracyclinones possessing anticancer activity.<sup>8</sup>

In principle, this isomerization can proceed *via* three alternative pathways: (1) formation (at the initial moment) of only complex **1**, which then spontaneously or catalytically isomerizes to complex **2**; (2) partial isomerization of the 1,4-dihydronaphthalene ligand to 1,2-dihydronaphthalene under the action of  $(\text{NH}_3)_3\text{Cr(CO)}_3$  or  $\text{Py}_3\text{Cr(CO)}_3$  as catalysts followed by the interaction of both ligands with the chromium complex and formation of a mixture of compounds **1** and **2**; (3) isomerization of an intermediate chromium tricarbonyl complex of unknown structure (formed at the initial moment along with complex **1**), which is further rearranged to complexes **1** and **2**. It should be kept in mind that the thermal isomerization of 1,4-dihydronaphthalene itself to 1,2-dihydronaphthalene occurs under relatively drastic conditions (heating in chloronaphthalene at  $301^\circ\text{C}$ ) and rather slowly.<sup>9</sup> Catalytic isomerization of 1,4-dihydronaphthalene and its derivatives also requires special conditions and elevated temperatures, for example, heating of its melt for 8 h at  $140^\circ\text{C}$  in the presence of  $\text{Fe(CO)}_5$  (see Ref. 8) or contact with alumina or zeolites in the gaseous phase at temperatures higher than  $200^\circ\text{C}$ .<sup>10</sup> In addition, we showed in special experiments that complex **1** is stable at temperatures below  $100^\circ\text{C}$  and is not rearranged to complex **2**, including the reaction in the presence of other chromium tricarbonyl complexes as possible catalysts.

In our opinion, these facts indicate in favor of ligand isomerization in some complex of unknown structure, for

instance, due to hydride shifts involving a metal. We believe that this complex could be formed at the initial stage due to the oxidative addition of the tricarbonylchromium group to the cyclohexadiene ring and hydrogen atom shift from one of the  $\text{sp}^3$ -hybridized carbon atoms to the chromium atom to form hydride **3** with the  $\eta^5$ -structure (Scheme 2). In the next step, the tricarbonylchromium group in intermediate complex **3** is irreversibly transferred to the aromatic ring with abstraction of the hydrogen atom, which migrates to the 1-*endo*- or 2-*endo*-position of the cyclohexadiene ring to form complexes **1** and **2**, respectively.

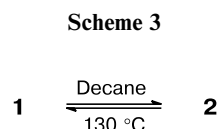


*i.*  $(\text{NH}_3)_3\text{Cr(CO)}_3$  or  $\text{Py}_3\text{Cr(CO)}_3$ .

Heating of pure complex **1** in decane for 16 h at  $130^\circ\text{C}$  produces a mixture of complexes **2** and **1** in a ratio of 19 : 1 ( $^1\text{H}$  and  $^{13}\text{C}$  NMR data). Further heating of this mixture induces no change in the ratio of the components, being thus equilibrium for isomerization  $\textbf{1} \rightleftharpoons \textbf{2}$  at this temperature. On heating complex **1** under milder conditions ( $115^\circ\text{C}$ ), the ratio **2** : **1** is 60 : 40 after 24 h and only after 100 h it reaches 93 : 7, which is probably close to the equilibrium value at this temperature.

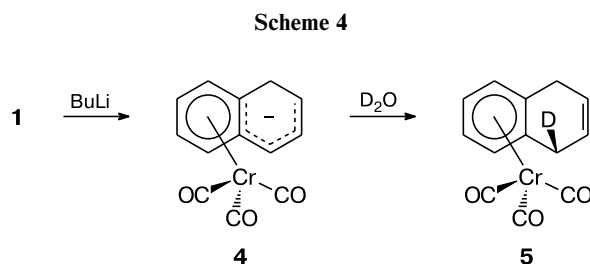
Complex **2** begins to rearrange with a noticeable rate to complex **1** only at temperatures above  $170^\circ\text{C}$ , which is related, most likely, to a higher activation energy of the backward process. In this case, only trace amounts of compound **1** are observed ( $\sim 5\%$  is the sensitivity limit of the NMR method). Unfortunately, we failed to measure the content of complex **1** in the equilibrium mixture and calculate the equilibrium constant because of considerable decomposition of the both complexes at so high temperature.

The presented data show that we found the thermally induced reversible rearrangement of isomeric ( $\eta^6$ -dihydronaphthalene)chromium tricarbonyl complexes **1** and **2** (Scheme 3).



In these complexes, hydrogen atom shifts can occur during isomerization, in principle, involving a transition metal atom or without it. As known, in the first case, this isomerization of cyclic dienes (for example, in the iron complexes with cyclohexadiene derivatives<sup>11</sup>) includes consecutive hydrogen atom shifts through a metallo-hydride intermediate. The main method for determination of transition metal participation in the hydride shifts is the study of rearrangements of the deuterated complexes, and the criterion of metal atom participation in the process is migration of the *endo*-hydrogen atoms (which can easily be established using deuterated compounds) and no migration of the *exo*-atoms.<sup>11</sup>

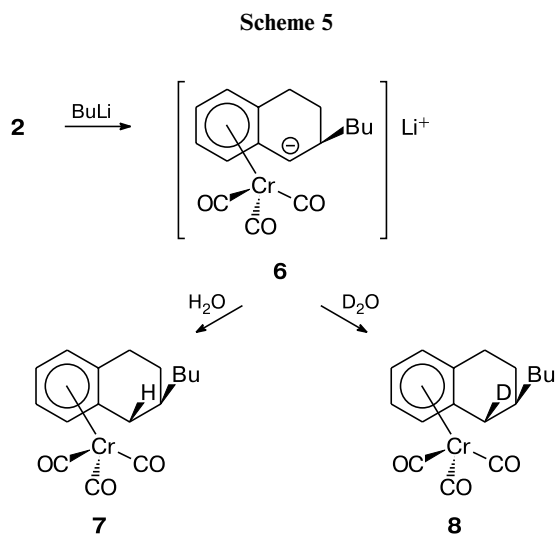
Therefore, we studied a possibility of selective introduction of the deuterium atom into compounds **1** and **2**. For this purpose, complex **1** was deprotonated using Bu<sup>n</sup>Li at  $-70\text{ }^{\circ}\text{C}$  in THF. It is well known<sup>12</sup> that, in similar cases, the chromium tricarbonyl complexes are deprotonated to the benzylic sp<sup>3</sup>-hybridized carbon atom activated by the presence of the strong electron-withdrawing Cr(CO)<sub>3</sub> group in the adjacent benzene ring. This affords anion **4**, whose formation was monitored by IR spectroscopy in the region of  $\nu(\text{CO})$ . The bands of the initial compound **1** (1960, 1883 cm<sup>-1</sup>) disappear, and new bands of anion **4** (1902, 1823, 1807 cm<sup>-1</sup>) appear with the characteristic low-frequency shift due to the appearance of the negative charge in the non-aromatic six-membered ring and with splitting of the low-frequency band due to a decrease in the C<sub>3v</sub> symmetry of the Cr(CO)<sub>3</sub> group to C<sub>s</sub> (Scheme 4)<sup>13</sup>.



As it is commonly met in these cases, the electrophilic species attacks anion **4** from the side opposite to the tricarbonylchromium group.<sup>14</sup> In fact, its treatment with D<sub>2</sub>O at  $-70\text{ }^{\circ}\text{C}$  affords mono-*exo*-deuterated complex **5** (degree of deuteration 95% (<sup>1</sup>H NMR and mass spectrometric data)) in 85% yield. The *exo*-position of deuterium was confirmed by comparison of the <sup>1</sup>H and <sup>2</sup>H NMR spectra (C<sub>6</sub>D<sub>6</sub>) for compounds **1** and **5**. In the <sup>1</sup>H NMR spectrum of compound **1**, the signals of the *exo*-hydrogen atoms lie in a higher field relative to the signal of the *endo*-atoms (ASIS effect<sup>2,14</sup>). On going to complex **5**, the intensity of the upfield signal from the *exo*-protons in the AA'BB' part of the complicated AA'BB'CC' system of the *exo*- and *endo*-protons H(1) and H(4) and vinylic

protons in positions 2 and 3 is halved, and the <sup>2</sup>H NMR spectrum contains only one singlet at  $\delta$  2.48.

Complex **2** reacts with Bu<sup>n</sup>Li essentially differently: regioselective addition of Bu<sup>n</sup>Li to the double bond occurs instead of deprotonation. The Bu group is observed in position 2 (NOE data<sup>15</sup>) and, as follows from the general regularity for the chromium tricarbonyl complexes, should be *exo*-oriented relative to Cr(CO)<sub>3</sub>. The reaction course was monitored by IR spectroscopy from the disappearance of the bands of complex **2** (1963, 1883 cm<sup>-1</sup>) and the appearance of bands of the corresponding lithium derivative **6** (1900, 1824, 1809 cm<sup>-1</sup>). After treatment of the reaction mixture with H<sub>2</sub>O or D<sub>2</sub>O, hydrogen (or deuterium) is observed in the *exo*-position relative to the Cr(CO)<sub>3</sub> group and complexes **7** or **8** are formed, respectively (Scheme 5). The structures of complexes **7** and **8** (position and orientation of substituents) were determined by analogy to the known data on stereochemistry of MeLi addition to complex **2** (see Ref. 16) and confirmed by the data of <sup>1</sup>H and <sup>2</sup>H NMR, decoupling experiments, ASIS effect, and NOE measurements.



Deuterated complex **5** was subjected to thermal isomerization under mild conditions (115  $^{\circ}\text{C}$ , 20 h) in nonane. This temperature regime was chosen to prevent its decomposition and formation of paramagnetic admixtures resulting in considerable broadening of the lines in the NMR spectra. We detected the <sup>2</sup>H NMR spectra with stabilization of resonance conditions on <sup>19</sup>F nuclei (C<sub>6</sub>F<sub>6</sub>) of samples of complex **5** in benzene before and after heating (Fig. 1). The spectrum of the first sample contained only a singlet from the *exo*-deuterium atom in position 1 of complex **5**. The spectrum of the second sample exhibits, in addition to the above signal, signals from isotopomeric ( $\eta^6$ -1,2-dihydronaphthalene)chromium tricarbonyls **9** and **10** containing the deuterium atom in vinylic position 4 and homoallylic *exo*-position 1, respec-

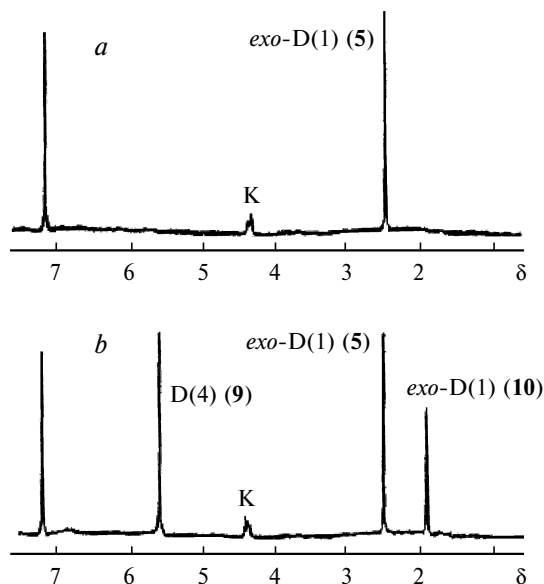


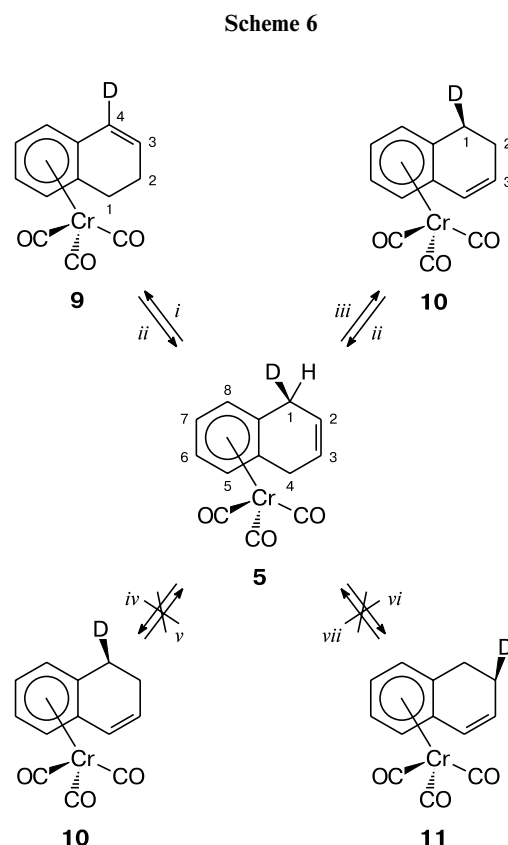
**Fig. 1.**  $^2\text{H}\text{--}\{^1\text{H}\}$  NMR spectra in benzene of sample **5** before heating (*a*) and of the sample being an equilibrium mixture of complexes **5**, **9**, and **10** after heating for 12 h at 130 °C in nonane (*b*) (K shows signals indicating the partial deuteration of complex **5** to the coordinated ring). The signal from the D nuclei (natural content) in benzene is observed at  $\delta$  7.15.

tively (see Fig. 1). The positions of the deuterium atom in isotopomers **9** and **10** were determined by the assignment in the  $^1\text{H}$  NMR spectrum of compound **2**, which was performed using the ASIS effect and NOE measurements.

The formation of complex **9** containing the deuterium atom in vinylic position 4 is explained by the 1,5-*endo*-hydride shift of the hydrogen atom from position 1 to position 3 in complex **5** (Scheme 6). Similar 1,5-*endo*-shift of the hydrogen atom but from position 4 to position 2 produces complex **10** containing the deuterium atom in the 1-*exo* position. The configuration of the hydrogen and deuterium atoms at the  $\text{sp}^3$ -hybridized carbon atoms in complexes **9** and **10** was confirmed using the data of  $^1\text{H}$  NMR spectroscopy, decoupling experiments, and NOE and ASIS effect measurements for complexes **1** and **2**. Integration of signals in the  $^2\text{H}$  NMR spectrum gives the **9** : **10** : **5** ratio equal to 42 : 23 : 35.

It can be concluded on the basis of the presented data that the described above transformations occur due to the 1,5-shifts of the only *endo*-hydrogen atoms.

It should be emphasized that migrations of the *exo*-hydrogen atoms, in principle, cannot result in the appearance of signals from the deuterium atoms in the vinylic position. It is characteristic that the  $^2\text{H}$  NMR spectrum exhibits no signals from isotopomeric ( $\eta^6$ -1,2-dihydronaphthalene)chromium tricarbonyl complex **11** containing the deuterium atom in the allylic 2-*endo*-position, which could be formed due to the 1,5-*exo*-D shift (see



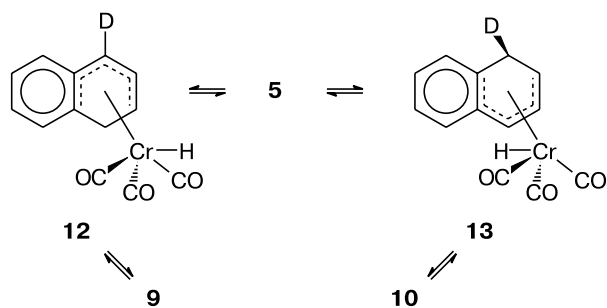
*i.* 1,5-*endo*-Shift of H atom from position 1. *ii.* 1,5-*endo*-Shift of H atom from position 2. *iii.* 1,5-*endo*-Shift of H atom from position 4. *iv.* 1,5-*exo*-Shift of H atom from position 4. *v.* 1,5-*exo*-Shift of H atom from position 2. *vi.* 1,5-*exo*-Shift of D atom from position 1. *vii.* 1,5-*exo*-Shift of D atom from position 2.

Scheme 6). If both the *endo*- and *exo*-hydrogen atoms migrated, then the spectrum of the equilibrium mixture would contain signals from all the four isotopomers **5**, **9**, **10**, and **11**.

The fact that isomerization  $\mathbf{1} \rightleftharpoons \mathbf{2}$  involves only the *endo*-hydrogen atoms and does not involve the *exo*-atoms indicates a special role of the chromium atom, which is manifested, as we assume, through the formation of hydride intermediates **12** and **13** of  $\eta^5$ -structure. They are formed from complexes **1** and **2** upon the migration of the  $\text{Cr(CO)}_3$  group to the cyclohexadienyl ring and capturing of the *endo*-hydrogen atom from the  $\text{sp}^3$ -hybridized C(1) or C(4) atom for complex **1** and C(2) for complex **2** (Scheme 7).

The transformations of the hydride intermediates are accompanied by the "ricochet" rearrangement,<sup>17</sup> being "recoil" of the tricarbonylchromium group backward into the aromatic ring and "throw off" of the hydrogen atom to one of the positions of the cyclohexadienyl ring.

Scheme 7



To confirm participation of the chromium atom in isomerization  $1 \rightleftharpoons 2$  and to study the mechanism of this reaction, we used quantum chemical calculations in the framework of the density functional theory.

### Quantum chemical calculations

The density functional theory (DFT) is known to describe well the geometric, conformational, and energy parameters of the chromium tricarbonyl complexes of polyaromatic ligands, such as naphthalene,<sup>18</sup> dibenzothiophene,<sup>19</sup> biphenylene,<sup>20</sup> and fluoranthene.<sup>21,22</sup> This method showed itself for description of the kinetic and thermodynamic parameters of several chemical reactions and processes that occur in the chromium tricarbonyl complexes (metallotropic and ricochet rearrangements, ligand elimination, complex formation, *etc.*).<sup>18–23</sup>

**Calculation of rearrangement  $1 \rightleftharpoons 2$ .** At the initial stage, we optimized initial complexes 1 and 2. Optimized structures 1 and 2 are shown in Fig. 2.

The energy for complex 1 is by 2.65 kcal mol<sup>−1</sup> higher than that for complex 2, which agrees with experiment,

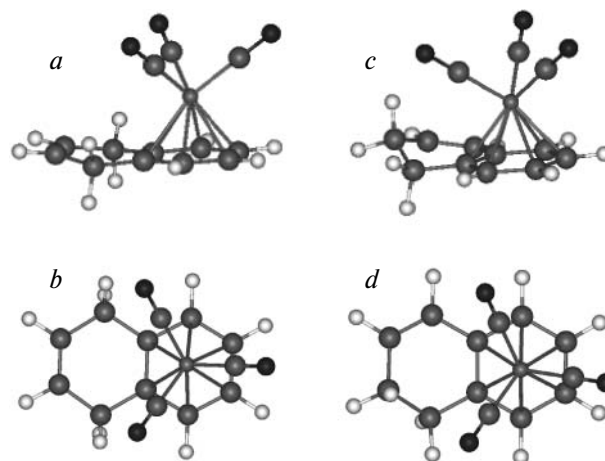


**Fig. 2.** Structures of compounds 1 (a, b) and 2 (c, d) optimized by the DFT method (side view (a, c) and view from above (b, d)).

according to which complex 2 prevails in equilibrium mixture  $1 \rightleftharpoons 2$  after rather prolong heating (thermodynamic control). The cyclohexadiene ring in compound 1 is strongly flattened, whereas in compound 2, as should be expected, it is non-planar to a great extent. In the both structures, the Cr(CO)<sub>3</sub> group is oriented relative to the arene ring in the same way as in an (η<sup>6</sup>-naphthalene)chromium tricarbonyl molecule.<sup>24</sup> The C—H bond lengths for the *exo*- and *endo*-hydrogen atoms are comparable, for complex 1 being 1.103 and 1.107 Å and for complex 2 1.099, 1.106 Å (C(1)—H) and 1.106, 1.099 Å (C(2)—H), respectively.

To check the hypothesis on chromium atom involvement in rearrangement  $1 \rightleftharpoons 2$ , we calculated the potential energy surface (PES) of migration of the tricarbonylchromium group from the benzene ring to the dihydrogenated cycle. This migration should occur during isomer-

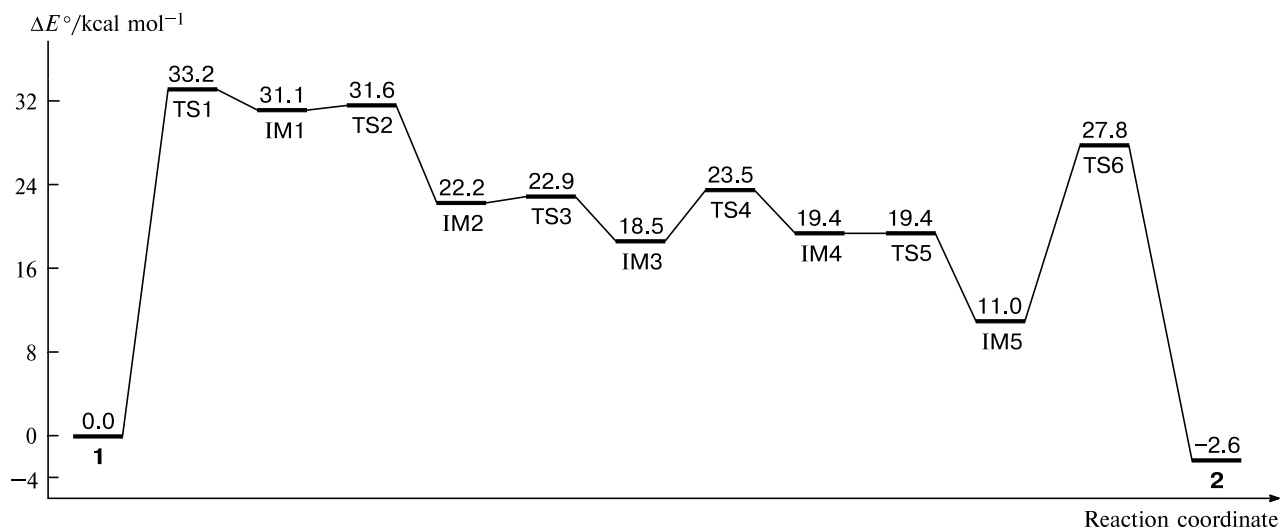


**Fig. 3.** Energy diagram of equilibrium rearrangement  $1 \rightleftharpoons 2$ .

ization for capturing the hydrogen atom from one of the  $\text{sp}^3$ -hybridized carbon atoms of the cyclohexadiene ring by the chromium atom to form the  $\text{Cr-H}$  bond followed by hydrogen atom transfer from the metal atom to the adjacent carbon atom, for instance, through rotation of the tricarbonylmethyl hydride group. The study revealed several transition states (TS) and intermediates (IM) on the PES for transformation  $1 \rightleftharpoons 2$ . The general energy diagram of this complicated process is presented in Fig. 3.

The first region corresponds to the formation of the unstable intermediate IM1 after surmounting a considerable barrier ( $33.2 \text{ kcal mol}^{-1}$ ). The structures of the tran-

sition state TS1 and intermediate IM1 are presented in Fig. 4, *a* and *b*.

It is characteristic that during the  $\text{TS1} \rightarrow \text{IM1}$  process, when the tricarbonylchromium group shifts, as should be expected, over the periphery of the ligand<sup>18–23</sup> toward the hexadienyl ring, the *endo*-hydrogen atom is brought together with the transition metal atom and the  $\text{C-H}_{\text{endo}}$  distance elongates. At the same time, the distances between the *exo*-hydrogen atom and transition metal atom and the  $\text{C-H}_{\text{exo}}$  distances change insignificantly. These changes can be interpreted as the formation of an agostic bond with the *endo*-hydrogen atom.<sup>4</sup> This agrees with

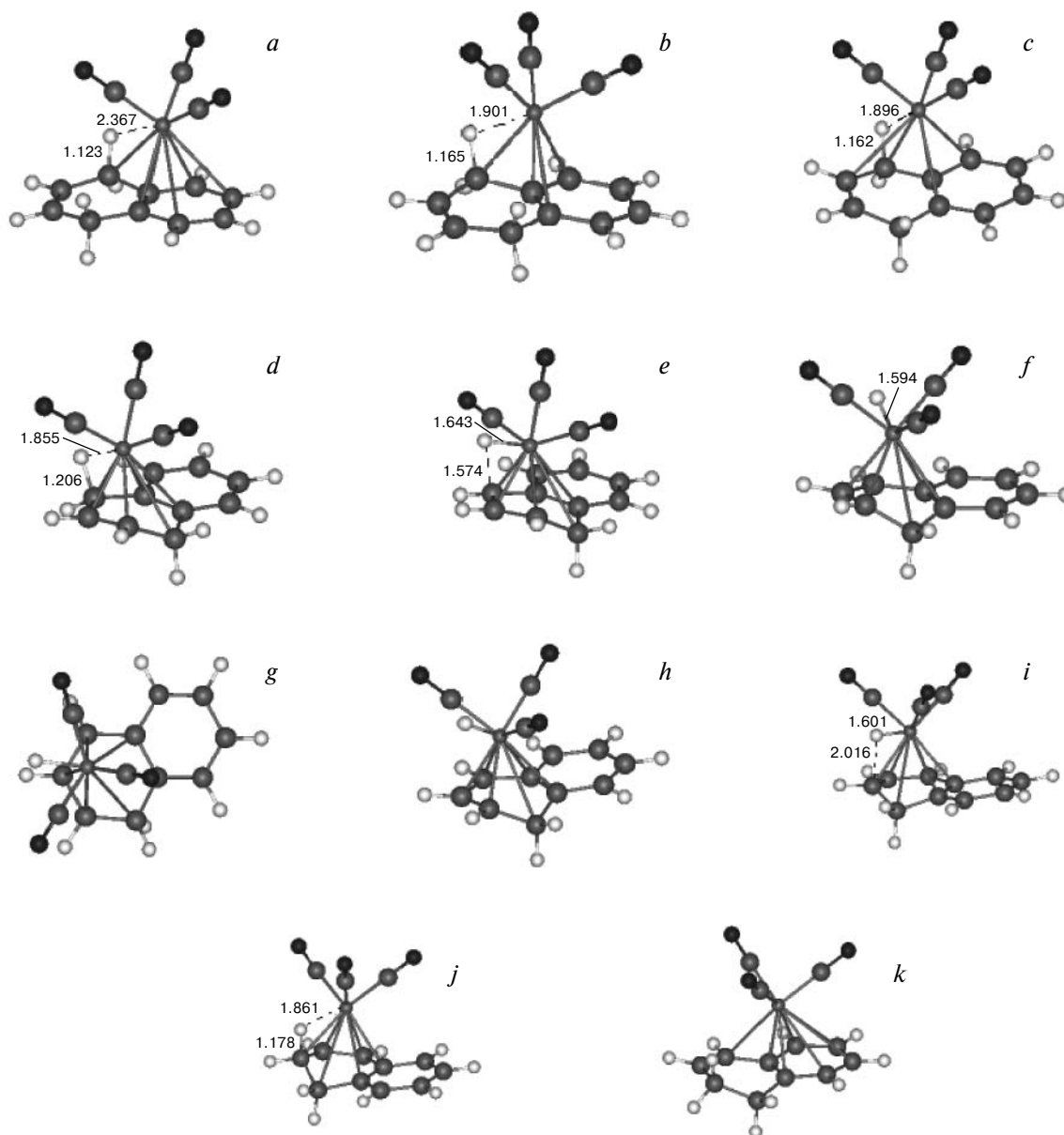


**Fig. 4.** Structures of the transition states TS1 (*a*), TS2 (*c*), TS3 (*e*), TS4 (*g*), TS5 (*i*), and TS6 (*k*) and intermediates IM1 (*b*), IM2 (*d*), IM3 (*f*), IM4 (*h*), and IM5 (*j*).

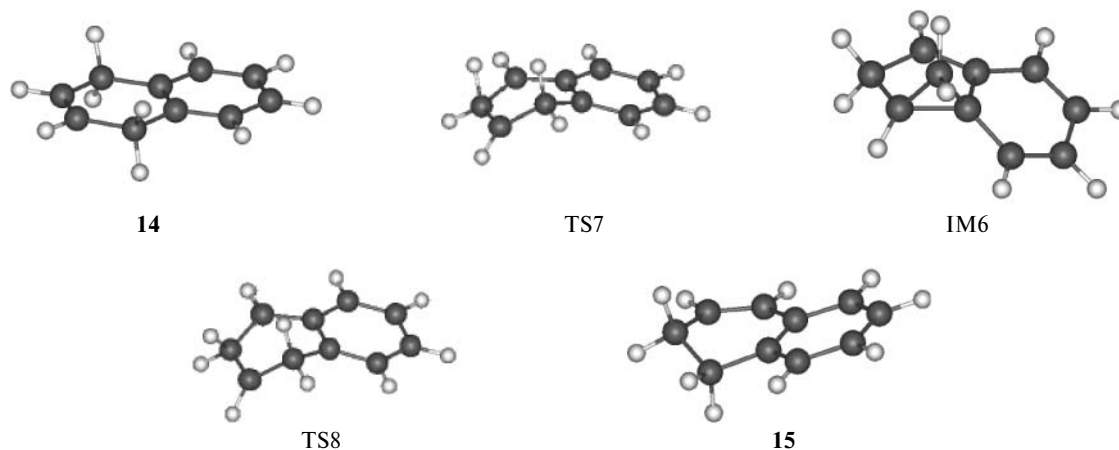


**Fig. 5.** Transition states TS7 and TS8 and intermediate IM6 of the rearrangement of 1,4-dihydronaphthalene (**14**) to 1,2-dihydronaphthalene (**15**).

available neutron diffraction data for the related complexes.<sup>25–28</sup>

The second region of the energy diagram is associated with the formation of the more stable intermediate IM2 after surmounting a low barrier (0.5 kcal mol<sup>−1</sup>). The structures of TS2 and IM2 are presented in Fig. 4, *c* and *d*. In this region, the agostic H—Cr bond is retained and the Cr(CO)<sub>3</sub> group is completely transferred to the dihydrogenated ring with a considerable stabilization of IM2.

The third region reflects the process of formation of the hydride intermediate IM3 after surmounting a low barrier (0.7 kcal mol<sup>−1</sup>). The structures of the transition state TS3 and intermediate IM3 are shown in Fig. 4, *e* and *f*.

The fourth region corresponds to the turn of the HCr(CO)<sub>3</sub> group and closing together of the hydride hydrogen and C(2) atoms. The corresponding structures of the transition state TS4 and intermediate IM4 are shown in 4, *g* and *h*.

The fifth region concerns the almost barrier-free formation of the intermediate IM5 and is characterized by hydride bond transformation back into the agostic bond. The corresponding structures of the transition state TS5 and intermediate IM5 are presented in Fig. 4, *i* and *j*.

Finally, the last region is related to the transfer of the Cr(CO)<sub>3</sub> group from the cyclohexadienyl to benzene ring, and for both TS6 and TS1 the tricarbonylchromium group is arranged at the periphery of the ligand (Fig. 4, *k*).

**Calculation of rearrangement of 1,4-dihydronaphthalene to 1,2-dihydronaphthalene.** It seems important to estimate the energy change for the alternative rearrangement mechanism involving no Cr(CO)<sub>3</sub> group. For this purpose, we calculate the hydride shift process in the corresponding free ligands during the transformation of 1,4-dihydronaphthalene (**14**) into 1,2-dihydronaphthalene (**15**). The calculation showed that the rearrangement proceeds with formation of the intermediate IM6 of cyclopropane structure through two transition states, namely,

TS7 and TS8. This result seems somewhat unusual, although the backward process of cyclopropane ring opening to form the double bond in the presence of the ruthenium complexes has been described.<sup>29</sup> The calculated structures are presented in Fig. 5. The corresponding energy diagram is shown in Fig. 6. The data obtained suggest that the ratio between compounds **14** and **15** under thermodynamic equilibrium conditions should be the same as that for complexes **1** and **2** but with a much higher energy barrier. Thus, ligand isomerization involving no transition metal requires much higher temperatures to achieve equilibrium in complete accord with the experimental data.<sup>9</sup>

**Calculation of alternative process of rearrangement  $1 \rightleftharpoons 2$ .** For completeness we calculated the transition state of the alternative process of rearrangement  $1 \rightleftharpoons 2$  in the complexes. As in the case of ligand isomerization, the alternative process occurs as shifts of hydro-

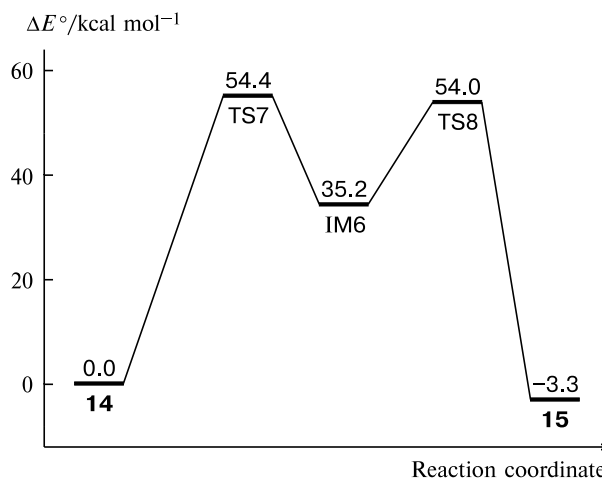


**Fig. 6.** Energy diagram of the rearrangement of 1,4-dihydronaphthalene (**14**) to 1,2-dihydronaphthalene (**15**).

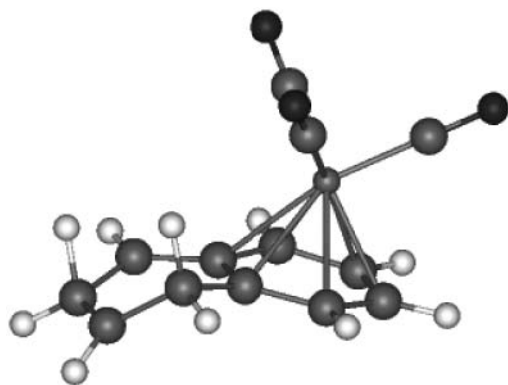


Fig. 7. Transition state for rearrangement  $1 \rightleftharpoons 2$  involving no chromium atom.

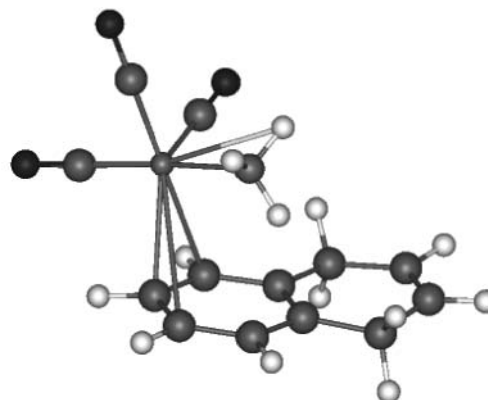
gen atoms involving no transition metal. However, the thermodynamic parameters for the shifts of the *endo*-hydrogen atoms only but without the chromium atom, *i.e.*, without the haptotropic transition of the tricarbonylchromium group to the dihydrogenated ring and without formation of the agostic and hydride intermediates were calculated. The structure of the transition state for this process is presented in Fig. 7. The barrier was  $56.6 \text{ kcal mol}^{-1}$ , which is by  $2.2 \text{ kcal mol}^{-1}$  higher than the barrier for isomerization of the ligands themselves in the absence of the tricarbonylchromium group.

We performed no calculations for the principally possible rearrangement through the shift of the *exo*-hydrogen atoms, because its energy barrier *a priori* should be comparable with two preceding values, *i.e.*, rather high.

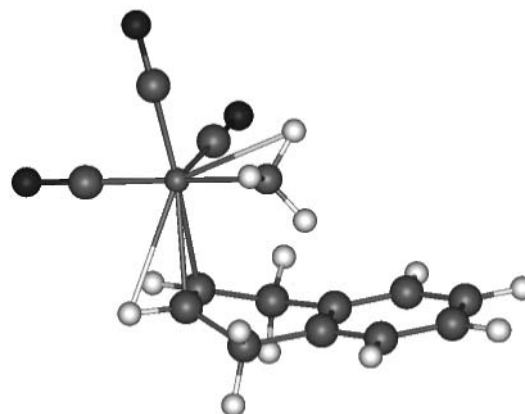
**Model of insertion of the  $\text{Cr(CO)}_3$  group into 1,4- and 1,2-dihydronaphthalenes.** According to the experimental data for coordination of the  $\text{Cr(CO)}_3$  group to 1,4-dihydronaphthalene, the reaction of the ligand with different complex chromium carbonyls in a wide temperature range affords a mixture of complexes **1** and **2**. At the same time, reaction of 1,2-dihydronaphthalene with  $\text{Cr(CO)}_3$  produces only isomer **2**.<sup>7</sup>

To understand a reason for different behavior of the isomeric ligands in complex formation, we simulated the step of attack of the considered ligands by the coordinately unsaturated particle  $(\text{NH}_3)\text{Cr(CO)}_3$ , *i.e.*, final step of formation of chromium tricarbonyl complexes **1** and **2** ("recoil" of the latter, additional ligand  $\text{NH}_3$  different from CO). We have earlier<sup>21</sup> used this approach successfully to explain the formation of the fluoranthene complex according to the "naphthalene" type due to "kinetic control." The structures of two calculated complexes of 1,4-dihydronaphthalene with localization of the  $\text{NH}_3\text{Cr(CO)}_3$  group at the aromatic (**16**) and dihydrogenated (**17**) rings are presented in Fig. 8.

Structure **17** is only by  $3.0 \text{ kcal mol}^{-1}$  more stable than structure **16**. Thus, complex formation in the penultimate



16



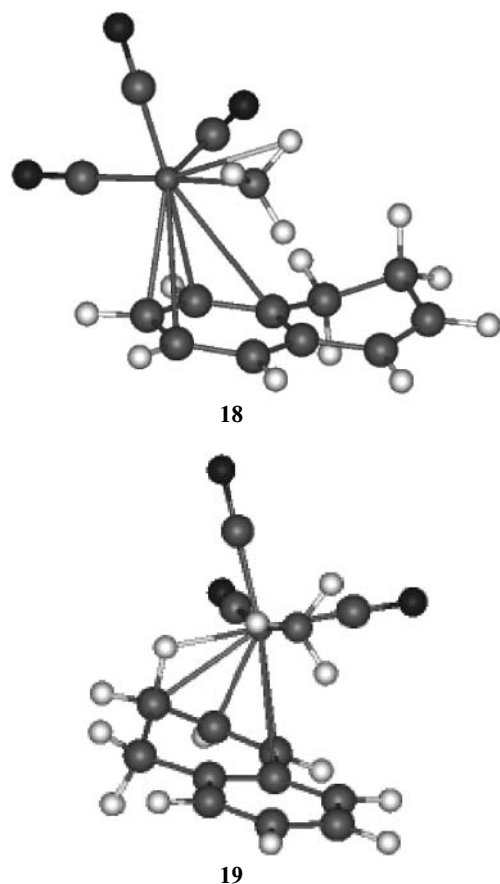
17

Fig. 8. Simulation of the tricarbonylchromation of 1,4-dihydronaphthalene (**14**): structures of calculated complexes **16** and **17**.

step proceeds, probably, to the dihydrogenated ring and partially to the aromatic ring. This, in turn, results in the situation when the elimination of the last ligand ( $\text{NH}_3$ ) from intermediate **16** produces stable complex **1** and unstable chromium tricarbonyl complexes situated in the region of the intermediates IM1–IM5 (see Fig. 3), which includes the hydride intermediate IM3 (formation of IM3 is also assumed during rearrangement  $1 \rightleftharpoons 2$  (see Scheme 7)). As seen from the diagram of the described above process of rearrangement  $1 \rightleftharpoons 2$  (see Fig. 3), the kinetic factor (difference in energies of TS1 and TS6, being  $5.4 \text{ kcal mol}^{-1}$ ) should result in the transformation of the intermediates IM1–IM5 mainly into isomer **2**. Thus, the presented results well explain the experimental fact of formation of a mixture of complexes **1** and **2**.

Somewhat different results were obtained by the simulation of the tricarbonylchromation of 1,2-dihydronaphthalene in the reaction with the coordinately unsaturated particle  $(\text{NH}_3)\text{Cr(CO)}_3$ . The structures of the two calculated complexes with coordination of the  $(\text{NH}_3)\text{Cr(CO)}_3$  group to the aromatic (**18**) and dihydrogenated (**19**) rings are presented in Fig. 9.





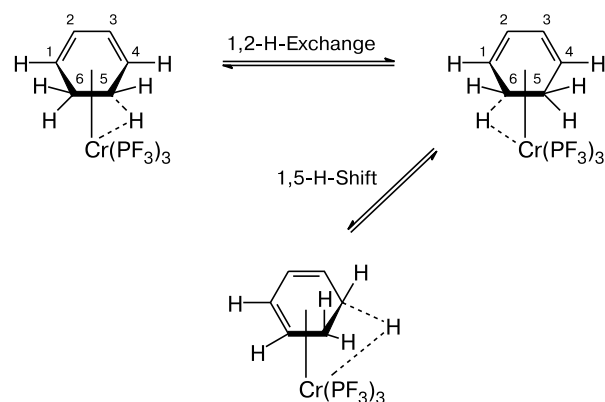
**Fig. 9.** Simulation of the tricarbonylchromation of 1,2-dihydronaphthalene (**15**): structures of calculated complexes **18** and **19**.

As in the case of the 1,4-dihydronaphthalene complex, the structure with coordination to the dihydrogenated ring turned out to be energetically more favorable (by 9.9 kcal mol<sup>-1</sup>). In this situation, the process is directed toward the predominant formation of complex **2** after elimination of the last ammonia molecule, regardless of the fact what factor (kinetic or thermodynamic) is prevailing. However, taking into account the conditions of synthesis of complex **2** (high temperature along with considerable duration of experiment),<sup>7</sup> we believe that thermodynamic equilibrium should be established. In this case, ~5% isomer **1** should be found if the experiment was carried out thoroughly. Its absence indicates, probably, that traces of complex **1** could be lost during purification procedures of product **2** (chromatography, recrystallization, *etc.*).

It should be mentioned that no kinetic measurements at different temperatures were carried out for isomerization **1**  $\rightleftharpoons$  **2** and, as a consequence, the activation energy of the process was not determined. However, the latter should be close to 30–35 kcal mol<sup>-1</sup>.<sup>18–22</sup> Many examples for hydride shifts in unsaturated cycles are described,<sup>4</sup>

but reliable quantitative data are virtually lacking. For hydride shifts in the chromium tricarbonyl and chromium trifluorophosphine complexes of cyclohexadiene, the activation energies of the 1,5-hydride shift and 1,2-hydride exchange, when the *endo*-protons at two adjacent sp<sup>3</sup>-hybridized carbon atoms alternatively become agostic, were determined<sup>30</sup> by dynamic NMR (Scheme 8). The <sup>1</sup>H NMR spectra and X-ray diffraction data indicate that the process is initiated by the chromium atom and proceeds through the hydride and agostic intermediates.<sup>30</sup>

**Scheme 8**



We chose these systems as model and performed the DFT calculations of their PES for two processes: 1,5-hydride shift and 1,2-hydride exchange, which is alternative agostic bond formation.

The optimized structures of the products and TS are shown in Fig. 10. The energy diagram of the both processes in the chromium trifluorophosphine complexes of cyclohexadiene is presented in Fig. 11. The presented data show that the PES of the 1,5-hydride shift contains both agostic complex **20** and hydride complex **21**, whose energy is by 3.85 kcal mol<sup>-1</sup> higher. They are separated with a barrier of 4.39 kcal mol<sup>-1</sup> related to TS9. The transition state TS10 corresponds to the turn of the Cr(PF<sub>3</sub>)<sub>3</sub> group to the next, degenerate hydride complex **21'**. Then agostic degenerate complex **20'** is formed through the transition state TS9'. The 1,2-exchange of the hydrogen atom between agostic degenerate complexes **20** and **20'** passes through the symmetric (*C<sub>s</sub>*) transition state TS11, which is by 1.77 kcal mol<sup>-1</sup> higher in energy than TS10.

The experimental data on the activation barriers for 1,2-exchange (7.8 kcal mol<sup>-1</sup>) and 1,5-shift (6.2 kcal mol<sup>-1</sup>) in the chromium trifluorophosphine hexadiene complexes somewhat differ from the calculated values (6.50 and 4.73 kcal mol<sup>-1</sup>, see Fig. 11).

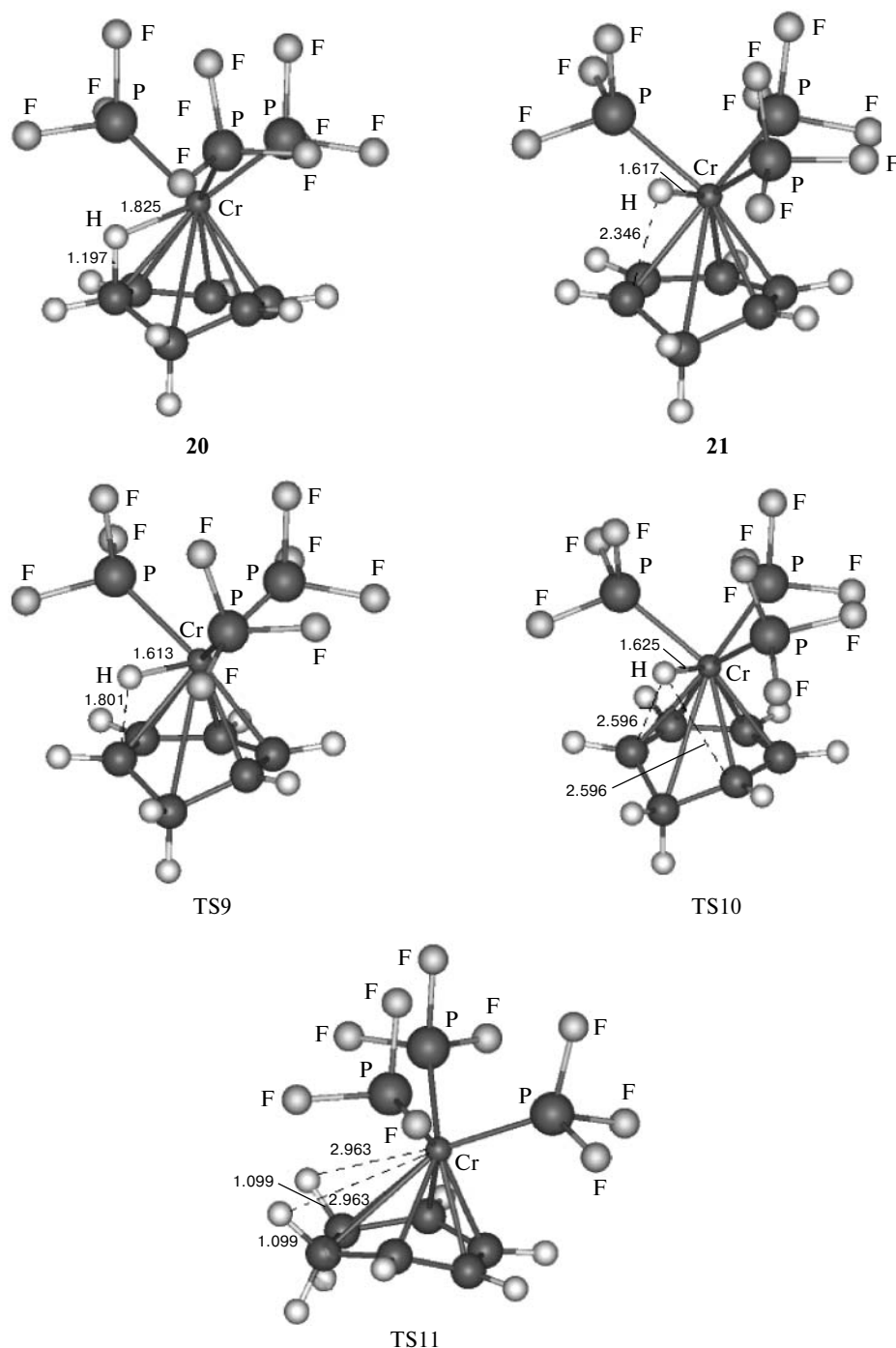


**Fig. 10.** Structures of products **20** and **21** and the transition states TS9–TS11 for the 1,5-shift and 1,2-exchange of the hydrogen atom in the chromium trifluorophosphine complexes of cyclohexadiene.

However, the process is qualitatively described adequately.

The qualitative pattern somewhat differs from the chromium tricarbonyl complexes: the activation barrier for the 1,5-shift is higher than that for the 1,2-exchange (Figs 12 and 13). Unfortunately, the corresponding experimental values were not measured.

It is noteworthy that the DFT calculation well described, as a whole, experimental data on the activation barriers of different transformations of organic compounds. This makes it possible to use in future the DFT method, as in the case of our investigation, to study dynamic processes in transition metal complexes with polycyclic aromatic compounds.

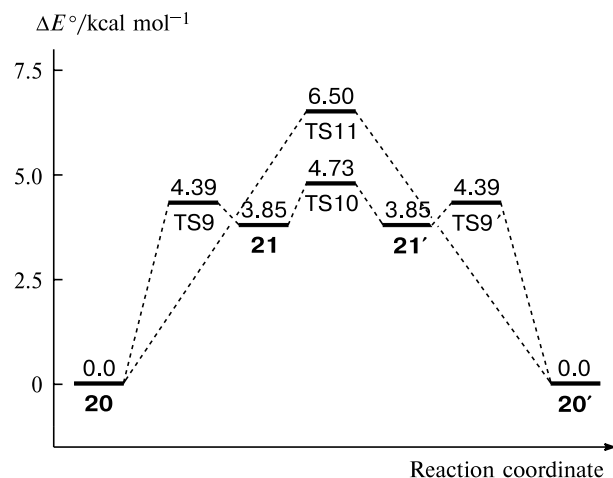


**Fig. 11.** Diagram of the 1,5-shift and 1,2-exchange of the hydrogen atom in the  $(\text{C}_6\text{H}_8)\text{Cr}(\text{PF}_3)_3$  complex (**20** and **20'** are the agostic complexes; **21** and **21'** are the hydride complexes; TS9, TS10, and TS9' are the transition states during 1,5-shift; TS11 is the transition state during 1,2-exchange).

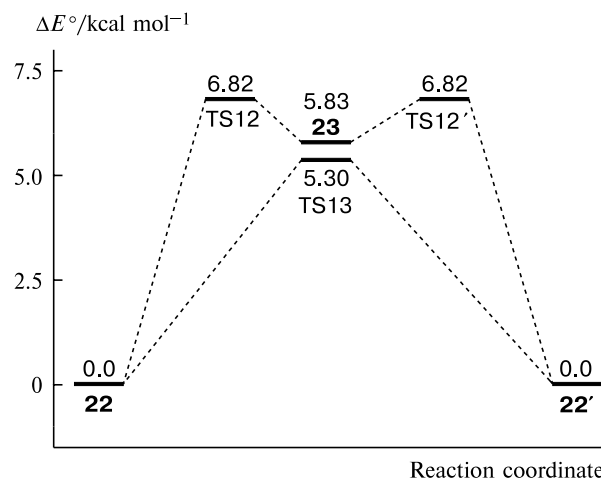


**Fig. 13.** Diagram of the 1,5-shift and 1,2-exchange of the hydrogen atom in the  $(\text{C}_6\text{H}_8)\text{Cr}(\text{CO})_3$  complex (**22** and **22'** are the agostic complexes; **23** is the hydride complex; TS12 and TS12' are the transition states during 1,5-shift; TS13 is the transition state during 1,2-exchange).

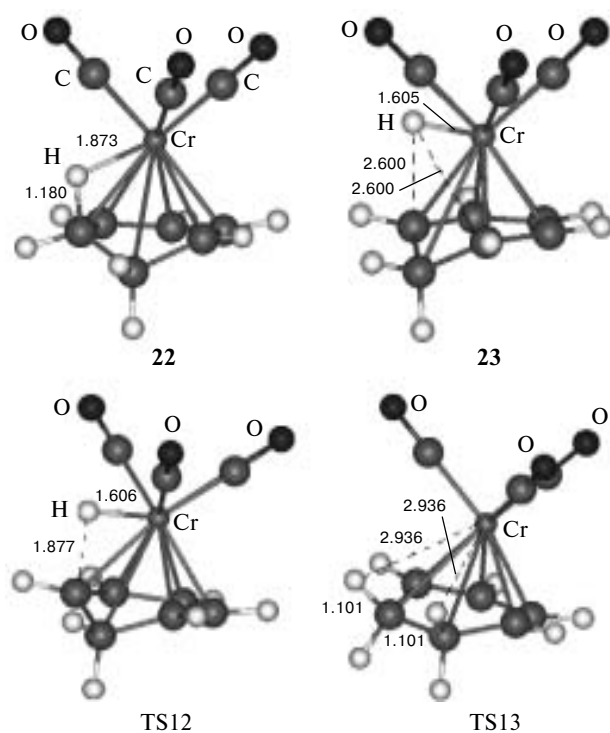


**Fig. 12.** Structures of products **22** and **23** and the transition states TS12 and TS13 for the 1,5-shift and 1,2-exchange of the hydrogen atom in the chromium tricarbonyl complexes of cyclohexadiene.

### Experimental

All procedures except TLC were carried out under argon purified from moisture and oxygen traces. Solvents were purified by prolong reflux over metallic sodium and distilled prior to

use. Tetrahydrofuran and diethyl ether were distilled from sodium benzophenone ketyl. Silica gel L 40/100  $\mu$  and Silufol (both from Chemapol) were used for preparative and analytical TLC, respectively. IR spectra were recorded on a UR-20 spectrometer (Carl Zeiss). NMR spectra were measured on a Varian VXR-400 spectrometer in a pulse mode. Difference NOE spectra were obtained for deaerated samples using the NOEDIF program accomplished in the spectrometer software. Mass spectra were recorded on a MAT Finnigan spectrometer (EI, 50 eV, 160  $^\circ\text{C}$ ).

**Synthesis of a mixture of compounds 1 and 2 through tris-pyridine complex  $\text{Py}_3\text{Cr}(\text{CO})_3$ .** Freshly distilled  $\text{BF}_3 \cdot \text{OEt}_2$  (17 g, 120 mmol) in ether (20 mL) was added at  $-30\text{ }^\circ\text{C}$  to a mixture of 1,4-dihydronaphthalene (4.49 g, 35 mmol) and  $\text{Py}_3\text{Cr}(\text{CO})_3$  (10 g, 26.8 mmol) in ether (150 mL). The temperature was slowly raised to  $25\text{ }^\circ\text{C}$  with stirring, and the mixture was stirred for additional 1 h. Then water was added to the reaction mixture. The solution was washed with water three times and dried over anhydrous  $\text{MgSO}_4$ . Ether was removed *in vacuo*, and the residue was chromatographed on a column (3 $\times$ 40 cm) with silica gel using a petroleum ether–benzene mixture as an eluent. A mixture of compounds **1** and **2** (2.96 g, 50%) was isolated from the orange zone after evaporation of the solvent and crystallization as fine orange crystals, m.p.  $115\text{--}123\text{ }^\circ\text{C}$ . Complexes **1** and **2** were separated by preparative TLC.

**Complex 1.** Found (%): C, 58.73; H, 3.72.  $\text{C}_{13}\text{H}_{10}\text{CrO}_3$ . Calculated (%): C, 58.65; H, 3.76.  $^1\text{H}$  NMR ( $\text{C}_6\text{D}_6$ ),  $\delta$ : 2.48 (m,  $\text{H}(1)_{\text{exo}}$ ,  $\text{H}(4)_{\text{exo}}$ ); 2.63 (m,  $\text{H}(1)_{\text{endo}}$ ,  $\text{H}(4)_{\text{endo}}$ ); 4.33–4.55 (m,  $\text{H}(5)\text{--H}(8)$ ); 5.44 (m,  $\text{H}(1)$ ,  $\text{H}(2)$ ).  $^{13}\text{C}$  NMR ( $\text{C}_6\text{D}_6$ ),  $\delta$ : 28.57 (C(1), C(4)); 91.50, 92.44 (C(5)–C(8)); 106.23 (C(4a), C(8a)); 123.97 (C(2), C(3)); 233.76 (CO). IR,  $\nu(\text{CO})/\text{cm}^{-1}$ : 1960, 1883. MS,  $m/z$  ( $I_{\text{rel}}$  (%)): 266 [ $\text{M}$ ] $^+$  (34), 238 [ $\text{M} - \text{CO}$ ] $^+$  (6.6), 210 [ $\text{M} - 2\text{CO}$ ] $^+$  (34.6), 182 [ $\text{M} - 3\text{CO}$ ] $^+$  (16), 130 [ $\text{C}_{10}\text{H}_{10}$ ] $^+$  (100), 52 [ $\text{Cr}$ ] $^+$  (67.8).

**Complex 2.**  $^1\text{H}$  NMR ( $\text{C}_6\text{D}_6$ ),  $\delta$ : 1.72 (m,  $\text{H}(3)_{\text{exo}}$ ); 1.95–2.20 (m,  $\text{H}(4)_{\text{exo}}$ ,  $\text{H}(4)_{\text{endo}}$ ); 4.38–4.58 (m,  $\text{H}(5)\text{--H}(8)$ ); 5.63 (m,  $\text{H}(1)$ ,  $\text{H}(2)$ ).  $^{13}\text{C}$  NMR ( $\text{C}_6\text{D}_6$ ),  $\delta$ : 22.83, 25.94 (C(3),

C(4)); 90.93, 91.28, 91.75, 93.14 (C(5)—C(8)); 102.75, 107.76 (C(4a), C(8a)); 124.07, 132.29 (C(1), C(2)). IR,  $\nu(\text{CO})/\text{cm}^{-1}$ : 1963, 1883. MS,  $m/z$  ( $I_{\text{rel}}$  (%)): 266  $[\text{M}]^+$  (28), 238  $[\text{M} - \text{CO}]^+$  (10.2), 210  $[\text{M} - 2 \text{CO}]^+$  (44), 182  $[\text{M} - 3 \text{CO}]^+$  (18), 130  $[\text{C}_{10}\text{H}_{10}]^+$  (100), 52  $[\text{Cr}]^+$  (71.3). The spectral data correspond to literature data.<sup>7</sup>

**Synthesis of deuterated complex 5.** A solution of compound **1** (0.2 g, 0.75 mmol) in THF (30 mL) was treated with twofold excess  $\text{Bu}^n\text{Li}$  in hexane at  $-70^\circ\text{C}$ . The temperature was raised to  $-50^\circ\text{C}$  with stirring, and the reaction mixture turned dark red. After 15-min stirring, the reaction mixture was treated with excess  $\text{D}_2\text{O}$  (Aldrich, 99.96% D) dissolved in THF to prevent freezing, and the mixture was stirred for additional 30 min. Complex **5** was obtained in a yield of 0.18 g (90%). MS,  $m/z$  ( $I_{\text{rel}}$  (%)): 267  $[\text{M}]^+$  (26), 239  $[\text{M} - \text{CO}]^+$  (12.1), 211  $[\text{M} - 2 \text{CO}]^+$  (42), 183  $[\text{M} - 3 \text{CO}]^+$  (20), 131  $[\text{C}_{10}\text{H}_9\text{D}]^+$  (100), 52  $[\text{Cr}]^+$  (70.3). According to data of the mass spectrum, the degree of deuteration was 95%.

**Synthesis of complex 7.** A solution of compound **2** (0.2 g, 0.75 mmol) in THF (30 mL) was treated with twofold mole excess  $\text{Bu}^n\text{Li}$  in hexane at  $-70^\circ\text{C}$ . The temperature was raised to  $-50^\circ\text{C}$  with stirring, and the reaction mixture turned red. After 15-min stirring, the reaction mixture was treated with excess  $\text{H}_2\text{O}$  dissolved in THF to prevent freezing, and the mixture was stirred for additional 30 min. Complex **7** was obtained in a yield of 0.15 g (63%). Found (%): C, 63.15; H, 6.25.  $\text{C}_{17}\text{H}_{20}\text{CrO}_3$ . Calculated (%): C, 62.96; H, 6.17.  $^1\text{H}$  NMR ( $\text{C}_6\text{D}_6$ ),  $\delta$ : 0.73, 1.42, 1.54, 1.65, 2.00, 2.28, 2.42 (all m,  $\text{H}(1)_{\text{exo}}-\text{H}(4)_{\text{exo}}$ ,  $\text{H}(1)_{\text{endo}}-\text{H}(4)_{\text{endo}}$ ); 0.88 (t, Me,  $J = 7.15$  Hz); 1.02, 1.12, 1.22 (all m,  $(\text{CH}_2)_3$ ); 4.45 (m,  $\text{H}(5)-\text{H}(8)$ ).  $^{13}\text{C}$  NMR ( $\text{C}_6\text{D}_6$ ),  $\delta$ : 14.25, 23.19, 27.21, 28.62 ( $\text{Me}(\text{CH}_2)_3$ ); 29.08, 33.08, 35.32, 35.90 (C(1)—C(4)); 91.45, 91.73, 93.54, 93.62 (C(5)—C(8)); 108.33, 109.78 (C(4a), C(8a)). IR,  $\nu(\text{CO})/\text{cm}^{-1}$ : 1962, 1884. MS,  $m/z$  ( $I_{\text{rel}}$  (%)): 324  $[\text{M}]^+$  (19), 296  $[\text{M} - \text{CO}]^+$  (10.1), 268  $[\text{M} - 2 \text{CO}]^+$  (48), 240  $[\text{M} - 3 \text{CO}]^+$  (28), 188  $[\text{C}_{14}\text{H}_{20}]^+$  (100), 52  $[\text{Cr}]^+$  (70.3).

**Synthesis of complex 8.** A solution of complex **2** (0.1 g, 0.37 mmol) in THF (17 mL) was treated with twofold mole excess  $\text{Bu}^n\text{Li}$  in hexane at  $-70^\circ\text{C}$ . The temperature was raised to  $-50^\circ\text{C}$ , and the reaction mixture turned red. After 15-min stirring, the reaction mixture was treated with excess  $\text{D}_2\text{O}$  dissolved in THF to prevent freezing, and the mixture was stirred for additional 30 min. Complex **8** was obtained in a yield of 0.06 g (52%). MS,  $m/z$  ( $I_{\text{rel}}$  (%)): 325  $[\text{M}]^+$  (22), 297  $[\text{M} - \text{CO}]^+$  (12.5), 269  $[\text{M} - 2 \text{CO}]^+$  (33), 241  $[\text{M} - 3 \text{CO}]^+$  (28), 189  $[\text{C}_{14}\text{H}_{19}\text{D}]^+$  (100), 52  $[\text{Cr}]^+$  (70.3). According to data of the mass spectrum, the degree of deuteration was 90%.

**Thermal rearrangement  $1 \rightleftharpoons 2$ .** The rearrangement was carried out in deaerated decane or nonane. Individual complexes **1** or **2** separated by TLC were dissolved in a solvent heated to  $50^\circ\text{C}$  under dry purified argon, and heating was continued at a required temperature for a certain time. The course of rearrangement  $1 \rightleftharpoons 2$  was monitored by TLC without isolation of the pure complexes (complex **2** is yellow-colored and more mobile on TLC plate (silica gel, benzene—hexane (1 : 1) mixture as an eluent) than orange complex **1**) or by removal of decane on the silica gel layer using hexane (under these conditions, the complexes are not eluted), further washing of a mixture of the complexes with pentane, drying of the substance *in vacuo*, and  $^1\text{H}$  and  $^{13}\text{C}$  NMR analysis.

All DFT calculations were performed with the nonempirical non-local PBE functional<sup>31</sup> in the extended split TZ2p basis set using the PRIRODA complex program<sup>32</sup> on the MBC-15000 computer cluster at the Joint Supercomputer Center (Moscow). Corrections to zero-point vibrational energies were calculated in the harmonic approximation. The type of stationary points (minima and transition states on the PES) were determined by analysis of the Hessians. The reaction paths were constructed by the internal reaction coordinate (IRC) method.<sup>33</sup>

The authors are grateful to the Alexander von Humboldt Foundation (Bonn, Germany) for kindly presented computer hardware used in part for quantum chemical and spectral calculations.

## References

1. Yu. F. Oprunenko, *Usp. Khim.*, 2000, **69**, 8 [*Russ. Chem. Rev.*, 2000, **69** (Engl. Transl.)].
2. N. G. Akhmedov, S. G. Malyugina, V. I. Mstislavsky, Yu. F. Oprunenko, V. A. Roznyatovsky, and Yu. A. Ustynyuk, *Organometallics*, 1998, **17**, 4607.
3. K. J. Karel, M. Brookhart, and R. Aumann, *J. Am. Chem. Soc.*, 1981, **103**, 2695.
4. M. Brookhart, M. L. H. Green, and L. L. Wong, *Prog. Inorg. Chem.*, 1988, **36**, 1.
5. M. J. Foreman, P. L. Pauson, G. R. Knox, K. H. Todd, and W. E. Watts, *J. Chem. Soc., Perkin Trans. 2*, 1972, **9**, 1141.
6. Yu. F. Oprunenko, A. S. Batsanov, S. G. Malyugina, M. D. Reshetova, N. A. Ustynyuk, and Yu. A. Ustynyuk, *Organometallics*, 1994, **13**, 2284.
7. V. N. Kalinin, I. A. Cherepanov, and S. K. Moiseev, *J. Organomet. Chem.*, 1997, **536—537**, 437.
8. M. Uemura, T. Minami, and Y. Hayashi, *J. Chem. Soc., Chem. Commun.*, 1984, 1193.
9. G. B. Gill and S. Hawkins, *J. Chem. Soc., Chem. Commun.*, 1974, 742.
10. G. Arich, S. Volpe, and P. Alessi, *Chem. Ind. (Milan)*, 1970, **52**, 223.
11. K. J. Karel, M. Brookhart, and R. Aumann, *J. Am. Chem. Soc.*, 1981, **103**, 2695.
12. S. G. Davies, S. J. Coote, and C. L. Goosfellow, in *Adv. Met. Org. Chem.*, Ed. L. S. Liebeskind, Pergamon, 1991, **2**, 1.
13. N. A. Ustynyuk, B. V. Lokshin, Yu. F. Oprunenko, V. A. Roznyatovsky, Yu. N. Luzikov, and Yu. A. Ustynyuk, *J. Organomet. Chem.*, 1980, **202**, 279.
14. N. A. Ustynyuk, L. N. Novikova, V. K. Bel'skii, Yu. F. Oprunenko, S. G. Malyugina, and Yu. A. Ustynyuk, *J. Organomet. Chem.*, 1985, **294**, 31.
15. D. Neuhaus and M. P. Williamson, *The Nuclear Overhauser Effect in Structural and Conformational Analysis*, VCH, Weinheim, 1989.
16. M. F. Semmelhack, W. Seifert, and L. Keller, *J. Am. Chem. Soc.*, 1980, **102**, 6586.
17. O. I. Trifonova, E. A. Ochertyanova, N. G. Akhmedov, V. A. Roznyatovsky, D. N. Laikov, N. A. Ustynyuk, and Yu. A. Ustynyuk, *Inorg. Chim. Acta*, 1998, **280**, 328.

18. Yu. F. Oprunenko, N. G. Akhmedov, S. G. Malyugina, V. I. Mstislavsky, V. A. Roznyatovsky, D. N. Laikov, Yu. A. Ustynyuk, and N. A. Ustynyuk, *J. Organomet. Chem.*, 1999, **583**, 136.
19. M. V. Zabalov, I. P. Gloriov, Yu. F. Oprunenko, and D. A. Lemenovskii, *Izv. Akad. Nauk, Ser. Khim.*, 2003, 1484 [*Russ. Chem. Bull., Int. Ed.*, 2003, **52**, 1567].
20. Yu. Oprunenko, I. Gloriov, K. Lyssenko, S. Malyugina, D. Mityuk, V. Mstislavsky, H. Günther, G. von Firks, and M. Ebener, *J. Organomet. Chem.*, 2002, **656**, 27.
21. Yu. Oprunenko, S. Malyugina, A. Vasil'kov, K. Lyssenko, Ch. Elschenbroich, and K. Harms, *J. Organomet. Chem.*, 2002, **641**, 208.
22. I. P. Gloriov, A. Yu. Vasil'kov, Yu. F. Oprunenko, and Yu. A. Ustynyuk, *Zh. Fiz. Khim.*, 2004, **78**, 313 [*Russ. J. Phys. Chem.*, 2004, **78**, 244 (Engl. Transl.)].
23. O. I. Trifonova, E. A. Ochertyanova, N. G. Akhmedov, V. A. Roznyatovsky, D. N. Laikov, N. A. Ustynyuk, and Yu. A. Ustynyuk, *Inorg. Chim. Acta*, 1998, **280**, 328.
24. V. Kunz and W. Nowacki, *Helv. Chim. Acta*, 1967, **50**, 1052.
25. J. M. Cole, V. C. Gibson, J. A. K. Howard, G. J. McIntyre, and G. L. P. Walker, *Chem. Commun.*, 1998, 1829.
26. R. Bau, S. A. Mason, B. O. Patrick, C. S. Adams, W. B. Sharp, and P. Legzdins, *Organometallics*, 2001, **20**, 4492.
27. W. T. Klooster, L. Brammer, C. J. Schaverien, and P. H. M. Budzelaar, *J. Am. Chem. Soc.*, 1999, **121**, 1381.
28. W. T. Klooster, R. S. Lu, R. Anwender, W. J. Evans, T. F. Koetzle, and R. Bau, *Angew. Chem., Int. Ed.*, 1998, **37**, 1268.
29. L. A. Paquette and R. Gree, *J. Organomet. Chem.*, 1978, **146**, 319.
30. E. P. Kündig, D. Amurrio, G. Bernardinelli, and R. Chowdhury, *Organometallics*, 1993, **12**, 4275.
31. J. P. Perdew, K. Burke, and M. Ernzerhof, *Phys. Rev. Lett.*, 1996, **77**, 3865.
32. D. N. Laikov and Yu. A. Ustynyuk, *Izv. Akad. Nauk, Ser. Khim.*, 2005, 804 [*Russ. Chem. Bull., Int. Ed.*, 2005, **54**, 820].
33. C. Gonzalez and H. B. Schlegel, *J. Phys. Chem.*, 1990, **94**, 5523.

*Received September 29, 2006;  
in revised form December 26, 2006*